CLASSIFICATION OF THE LCVF AVIRIS TEST SITE WITH A KOHONEN ARTIFICIAL NEURAL NETWORK

Erzsébet Merényi[1], Robert B. Singer[1] and William H. Farrand[2]

[1]University of Arizona, LPL, PIRL, Tucson, AZ 85721
[2]SAIC, 803 W Broad Street, Suite 100, Falls Church, VA 22046

1. BACKGROUND AND DATA

We are presenting a classification of an AVIRIS spectral image of the Lunar Crater Volcanic Field (LCVF) (Fig. 1.a). Geologic mapping from such data is made possible by distinctive mineral signatures: absorption features and the shape of the spectral continuum. The subtle spectral shape differences between some of the geological units in this scene along with the high dimensionality of the spectra presents a challenging pattern recognition task (Fig. 2.). We found an artificial neural network powerful in separating 13 geological units based on the full spectral resolution.

The LCVF, in northern Nye County, Nevada, was the primary focus of the NASA-sponsored Geologic Remote Sensing Field Experiment in the summer of 1989. It consists of over 100 square miles of Quaternary basaltic pyroclastic and flow deposits (Scott and Trask, 1971). These deposits lie atop ignimbrites and silicic lava flows of Tertiary age and in turn are overlain by Quaternary alluvial and playa deposits. This AVIRIS image was collected on September 29, 1989 at 11:44 PDT. The 256-by-256 pixel subsection in this study contains oxidized basaltic cinder deposits, the southern half of the Lunar Lake playa, and outcrops of the Rhyolite of Big Sand Spring Valley (mapped by Ekren et al., 1972). Vegetation in LCVF is sparse, but locally abundant within washes and near springs (Fig. 1.a).

2. CLASSIFICATION TECHNIQUE AND RESULTS

Artificial neural networks (ANN's) are parallel distributed computing architectures that learn to solve problems from examples. An introduction and overview can be found, for example, in (Pao, 1991). ANN's have proved powerful for the classification of complicated, noisy, real-life data (e. g., Huang and Lippman, 1987; Benediktsson *et al.* 1990; Hepner *et al.* 1990; Merényi *et al.* 1992). Many varieties of ANN's have been devised for different types of tasks. The most widely used paradigm is the Backpropagation, owing to its general applicability. Backpropagation, however, can be difficult to train, especially with large input vectors. Good training for the separation of classes with subtle differences may require a very high number of training samples. This could be problematic in remote sensing applications, because of limited field knowledge.

We used here a Kohonen-type Self-Organizing ANN combined with a categorization learning output layer (by NeuralWare, Inc., 1991). This first establishes a topological map of the cluster structure of the data in its 2-D hidden Kohonen layer (Kohonen, 1988), in an unsupervised regime. Then it is trained, in supervised mode, to assign class labels to the training patterns. The preformed clusters help keep the ANN from learning contradicting class labels by merely memorizing each case instead of deriving class properties. This can easily happen with a Backpropagation network when the number of training samples is small. Another advantage over Backpropagation is that the training is easier and much shorter. More details on how this ANN configuration works is given in Howell *et al.* (1993).

Approximately 30 training samples were selected for each of 13 spectral types (Fig. 2. left box) on the basis of spectral pattern differences and geological field knowledge. The data set consisted of 158 channels after the exclusion of spectrometer overlap, atmospheric water bands and excessively noisy channels. As explained on Fig. 2., the ANN produces reliable classification for all 13 classes, based on training with 0.6% of the image data. Corresponding geological maps (e. g., Scott and Trask, 1971) and field experiences confirm that each class is an identifiable geological unit in the test site. The 3 units that were mapped by earlier linear mixture modeling (Farrand and Singer, 1991), cinder, rhyolite and playa, are well matched and further broken down according to more subtle compositional differences which are in turn indicative of geologic processes (Fig. 1.b).

As little as 0.6% of the image data was sufficient for training to produce the presented geological details with this ANN. An important advantage of the Self-Organizing neural network over the most commonly used Back-propagation is that it achieves higher classification accuracy on test data based on a small amount of training data (e. g., Benediktsson *et al.* 1990). This enables very cost-effective sampling of remote sensing sites.

Acknowledgements: The computing facilities of the Lunar and Planetary Laboratory and the Planetary Image Research Laboratory, of the University of Arizona, software support by James Winburn and contributions by NASA Space Grant Intern Trevor Laing are cheerfully acknowledged.

REFERENCES

Benediktsson, J. A., P. H. Swain, O. K. Ersoy and D. Hong, 1990, "Classification of Very High Dimensional Data Using Neural Networks", *IGARSS'90 10th Annual International Geoscience and Rote Sensing Symp.* Vol. 2. p. 1269,

Ekren, E.B., E.N. Hinrichs and G.L. Dixon, 1973, "Geologic map of the Wall quadrangle, Nye County, Nevada", USGS Misc. Geol. Inv. Map I-719, scale 1:48,000.

Farrand, W.H. and R.B. Singer, 1991, "Analysis of altered volcanic pyroclasts using AVIRIS data", *Proc. Third AVIRIS Workshop, JPL Publication 91-28*, Jet Propulsion Laboratory, Pasadena, Ca.

Hepner, G. F., T. Logan, N. Ritter, N. Bryant, 1990, "Artificial Neural Network Classification Using a Minimal Training Set: Comparision to Conventional Supervised Classification", *Photogrammetric Eng. & Remote Sensing*, Vol. 56, No. 4, pp. 469-473

Howell, E. S., E. Merényi, L. A. Lebofsky, 1993, "Using Neural Networks to Classify Asteroid Spectra", forthcoming, *JGR Planets*

Huang, W. and R. Lippman, 1987, "Comparisions Between Neural Net and Conventional Classifiers", *IEEE First International Conference on Neural Networks*, Vol. IV, San Diego, pp. 485-494.

Kohonen, T., 1988, *Self-Organization and Associative Memory*, Springer-Verlag, New York

Merényi, E., R. B. Singer, J. S. Miller, 1992, "Spectral Analysis of the Surface of Mars: Neural Network Classification of High Spectral Resolution Images", *Bull. A.A.S.*, 24 No. 3, p. 979

NeuralWare, Inc., 1991, *NeuralWorks Professional II Manual*

Pao, Y. H., 1989, *Adaptive Pattern Recognition and Neural Networks*, Addison-Wesley

Scott, D.H. and N.J. Trask, 1971, "Geology of the Lunar Crater Volcanic Field, Nye County, Nevada", USGS Prof. Paper 599-I.

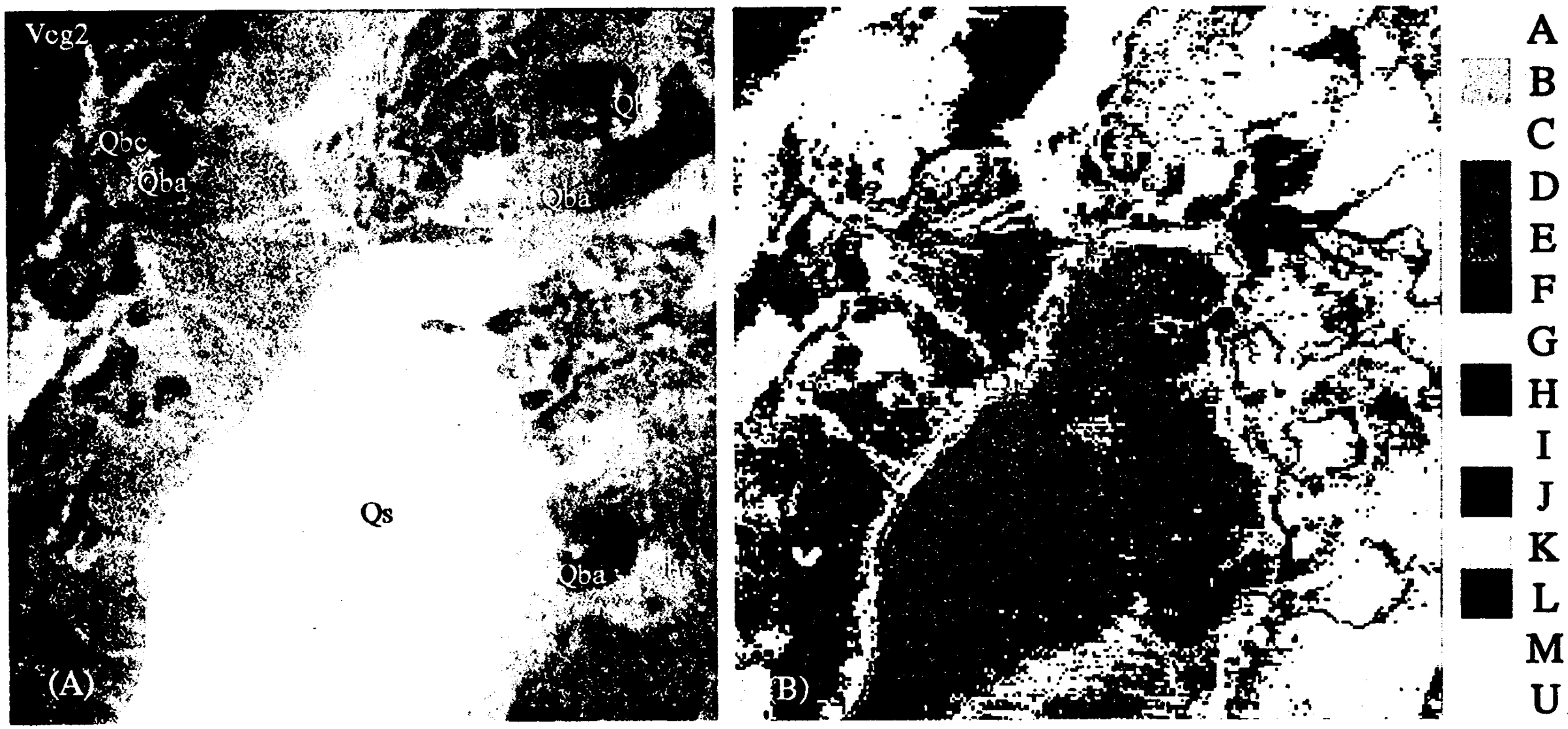

Figure 1. *a)* The LCVF study area. Labels mark some of the major geologic units based on the map by Scott and Trask (1971) and on our field knowledge. Qba - Basaltic ejecta aprons; Qb2 - Intermediate, black to gray weathered basalt; Qbc - Cinder cones; Qs - Sedimentary deposits; Ti - Ignimbrite and rhyolite flows, rhyolitic to andesitic; sequence. Veg1 - grass; Veg2 - scrub brush;

b) Classification map, produced by a self-organizing ANN. (See also Slide 5, in color, for better distinction between classes.)
A - highly oxidized cinders; B - rhyolite of Big Sand Springs Valley; C - vegetation type 1, probably grass; D - southern playa; E - northern playa (clay-rich); F - young basalt flows; G - Shingle Pass Tuff; H - Quaternary alluvium derived from silicic volcanics; I - old basalt flow; J - vegetation type 2, probably scrub brush; K - basalt cobbles on playa surface; L - ferric oxide rich soil; M - poorly oxidized dark cinders; U - unclassified (~10% of the pixels). Geologic maps confirm that these 13 classes correspond to known geologic units. The 3 endmember features mapped by earlier linear mixing modeling, cinder, rhyolite and playa, are covered and further refined by our 3 different cinder units (A, L and M), rhyolite (B), and southern and northern playa units (D and E), respectively. In addition, the ANN can separate two different vegetation types (C, J) from each other and from class B (rhyolite). These spectra are similar enough (see Fig. 2.) to cause singularity problems for linear inversion methods.

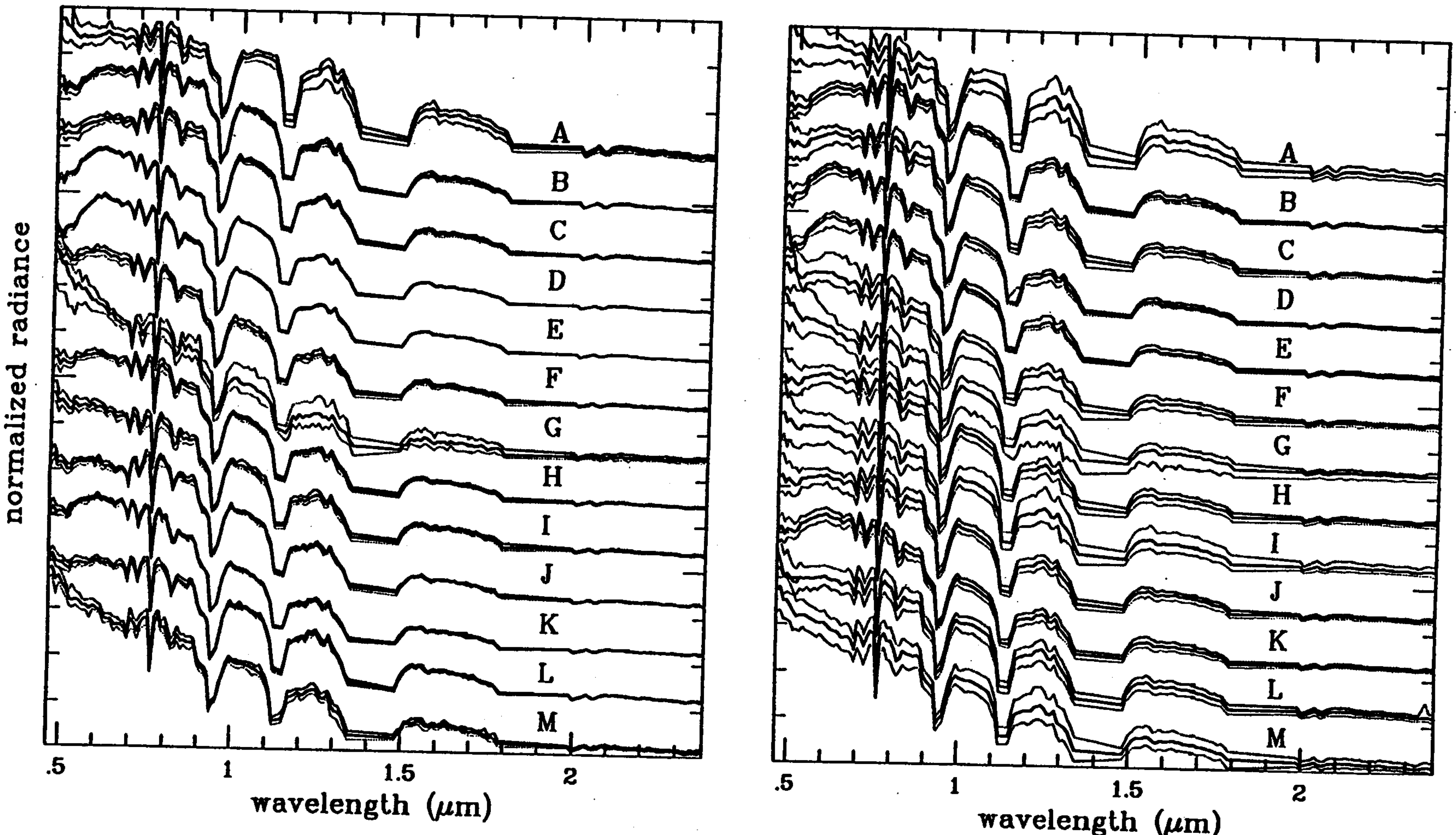

Figure 2. Comparision of the training spectra with the classification results. *Left:* Mean spectrum and the envelope of the training spectra for each class. The samples were taken from the radiance image, which was previously brightness normalized to cancel illumination geometry and albedo effects and thus retain only the spectral characteristics. Each training set contains only about 30 spectra. The water absorption bands were excluded from the analysis.

Right: Mean spectrum and the envelope of the extremes for each of the spectral classes A - M on Figure 1.a, produced by the neural network after it was trained on the samples shown in the left box. As seen, the mean spectra of these classes very closely match the mean spectra of the training sample sets. Quantitative evaluation shows that the relative difference between class and sample means is within 1% for classes B, D and E, between 5 - 10% for classes C and F - M, and between 5 - 20% for class A.